

Non-invasive Measurement of Vitreous Humor Stiffness in the Mouse using MR Elastography

E. H. Clayton¹, Q. Wang¹, S. K. Song², and P. V. Bayly^{1,3}

¹Mechanical Aerospace & Structural Engineering, Washington University in St. Louis, Saint Louis, MO, United States, ²Radiology/Radiological Sciences, Washington University in St. Louis, Saint Louis, MO, United States, ³Biomedical Engineering, Washington University in St. Louis, Saint Louis, MO, United States

Introduction

In vivo, non-invasive measurements of the stiffness (elastic modulus) of biological tissue can be performed with magnetic resonance elastography (MRE) [1]. Many studies have illustrated the versatility of MRE; stiffness estimates have been obtained from liver, muscle, breast, brain and heart [2-5]. Tissue health or disease is often indicated by its stiffness. In many cases tissue health is determined through invasive biopsy, which can subject the patient to discomfort and various risks. Non-invasive procedures, such as palpation, are qualitative, suffer from patient-to-patient variability, and are impossible in deep tissue. Furthermore, these measurements often only provide results in localized regions. However, with the continued development of MRE equipment and protocols, regional non-invasive measures of stiffness are becoming feasible in most soft tissues. In this study we demonstrate the measurement of loss and storage modulus of vitreous humor of the mouse eye using MR elastography non-invasively, *in vivo*.

Methods

Acquisition: MRE experiments were conducted using a Varian 4.7T small animal MRI scanner. Five male C57BL6 mice (Jackson Lab) were studied at three months of age. Mice were initially anesthetized with a single dose of Ketamine (87mg/kg) and Xylazine (13mg/kg). During scans anesthesia was administered continuously via subcutaneous infusion. Body temperature was maintained at 37°C and respiratory activity was monitored with a small animal heating and monitoring system (SA instruments, NY). All procedures were approved by the institutional Animal Studies Committee in accordance with the NIH Guide on the Care and Use of Animals. Each mouse was imaged with a custom-built mouse holder for eye imaging. A piezoceramic actuator (APA150M-NM, Cedrat Technologies) was mounted to a Delrin™ angle-section and positioned towards the inferior end of the mouse. A stinger extension with an eye-contacting “shear pad” was attached to the actuator to gently induce propagating shear waves into the eye through the cornea. A transistor-transistor logic (TTL) equipped function generator and low-current voltage amplifier were used to drive the actuator harmonically at 1200 Hz. Motion-encoding gradients were synchronized to actuator vibration to encode an isochromatic phase shift proportional to wave displacements, at four time points, using a custom phase-locked spin echo pulse sequence [6]. Two sets of motion-encoded data were acquired; one each with positive and negative motion encoding gradient polarity. Eye MRE data was obtained on a single trans-axial slice centered through the optical nerve. The acquired in-plane resolution was 100 x 100 μm²; through-plane resolution was 150 μm. TR/TE: 1000/27.5 ms and the number of MR motion encoding cycles (N_{MS}) was 5. Motion encoding gradients were sinusoidal with 15 G/cm amplitude. In this study, only through-plane displacements were sensitized, i.e. $u_z(x,y)$.

Data processing: The in-plane voxel dimension was interpolated to 50 x 50 μm²; through-plane voxel dimension remained 150 μm. Motion-sensitized phase contrast images were obtained by complex division of positive and negative polarity phase images. Phase contrast data was converted into displacements, $u_z(x,y,t)$, and the fundamental harmonic coefficient $U_z(x,y,\omega)$ was extracted by Fourier transform along the time dimension; both real and imaginary parts of $U_z(x,y,\omega)$ were retained. $U_z(x,y,\omega)$ was smoothed with a circular 6th-order Butterworth bandpass filter (in: 0.591 mm⁻¹, out: 1.58 mm⁻¹) in the spatial frequency domain. A central difference scheme was used to approximate the Laplacian; $\Delta^2 U_z(x,y,\omega)$. Inversion of the linear isotropic homogeneous material equation of motion, $(G' + iG'')\Delta^2 U_z(x,y,\omega) = -\rho\omega^2 U_z(x,y,\omega)$, was performed by local least squares fit. For each voxel, the complex modulus was found that minimizes the squared error between this equation and data from a 2-D kernel surrounding that voxel; the residual error of each fit, normalized by the variance in that kernel, was retained to assess “goodness-of-fit” of the linear isotropic homogeneous material model at that location. A normalized residual error (NRE) of zero would indicate a perfect local fit; a residual of 1.0 indicates a poor fit. All modulus approximations were thresholded; if the local model fit yielded an NRE > 0.5 the modulus was discarded and not used in subsequent summary calculations.

Results

Figure 1A,B shows the MRE imaging plane of interest and demarcates key features such as the actuated shear pad location. In Figure 1C unfiltered, uncropped, raw phase contrast data shows good wave penetration into the eye and surrounding tissue via gentle actuation of the cornea. The yellow arrow calls attention to what we believe is a wave reflection off of the retinal surface. A filtered and cropped wave displacement image is shown in Figure 1D. Representative storage (G') and loss (G'') modulus maps of mouse vitreous humor were overlaid onto anatomy images in Figure 1E,F. The storage modulus elastogram shows relatively good consistency of the modulus estimates over vitreous region. The mean storage and loss moduli of vitreous for all five mice were 895 +/- 122 Pa and 229 +/- 57 Pa, respectively.

Discussion

Results indicate that MRE measurement of vitreous humor is feasible in the mouse. Stiffness estimates are plausible; vitreous is significantly softer than mouse brain tissue [6], for example. A confining pressure acting within the eye and on the vitreous is likely to result in an increase in vitreous modulus. Accordingly this technique may be useful for diagnosis and evaluation of ocular disease.

References

[1] Muthupillai et al., Science, 1995, 269:1854-57; [2] Manduca et al., 2001, Med Image Anal, 5:237-54; [3] Sinkus et al., 2005, Magn Reson Med, 53:372-87; [4] Klatt et al., 2007, Phys. Med. Biol., 52:7281-94; [5] Robert et al., 2009, Magn Reson Med, 62(5):1155-63; [6] Atay et al., J Biomech Eng., 2008, 130(2):21013.

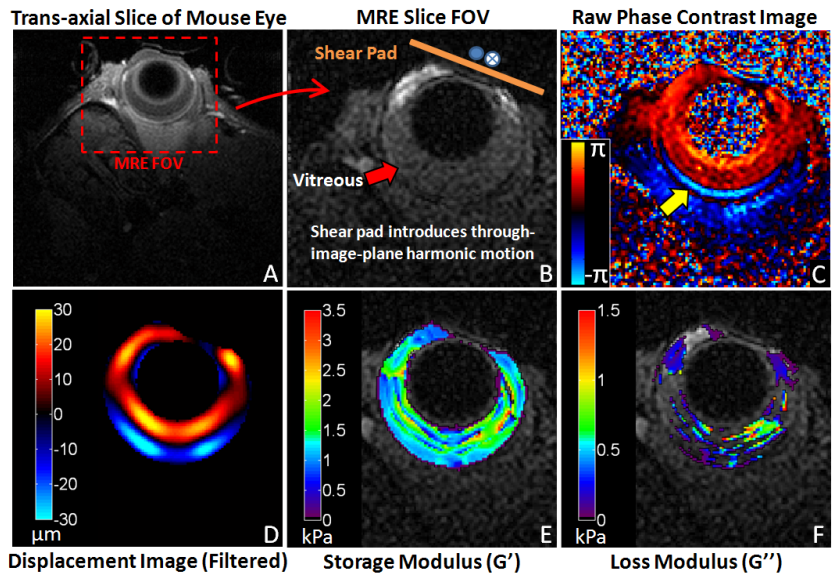


Figure 1: (A) High resolution MRI mouse eye, (B) Image FOV for eye MRE, (C) Raw, unfiltered, phase contrast data showing wave field, (D) Filtered imaginary fundamental harmonic of wave field, (E-F) Storage and loss moduli elastograms.